BJD
British Journal of Dermatology

Insights into male androgenetic alopecia using comparative transcriptome profiling: hypoxia-inducible factor-1 and Wnt/β-catenin signalling pathways*

Qingmei Liu,[1] Yulong Tang,[2] Yan Huang,[2] Ji'an Wang,[1] Kai Yang,[3] Yuting Zhang,[2] Weilin Pu,[2] Jing Liu,[2] Xiangguang Shi,[1] Yanyun Ma,[2] Chunya Ni,[3] Yue Zhang,[1] Yifei Zhu,[1] Haiyang Li,[1] Jiucun Wang,[1,2,4,5] Jinran Lin[1] and Wenyu Wu[1,3,6]

[1]Department of Dermatology, Huashan Hospital, Fudan University, Shanghai, China
[2]State Key Laboratory of Genetic Engineering, Collaborative Innovation Center for Genetics and Development, School of Life Sciences, and Human Phenome Institute, Fudan University, Shanghai, China
[3]Department of Dermatology, Jing'an District Central Hospital, Shanghai, China
[4]Institute of Rheumatology, Immunology and Allergy, Fudan University, Shanghai, China
[5]Research Unit of Dissecting the Population Genetics and Developing New Technologies for Treatment and Prevention of Skin Phenotypes and Dermatological Diseases, Chinese Academy of Medical Sciences (2019RU058), Shanghai, China
[6]Academy for Engineering and Technology, Fudan University, Shanghai, China

Linked Comment: M. Philpott. Br J Dermatol 2022; **187**:845.

Correspondence
Wenyu Wu.
Email: wuwenyu@huashan.org.cn

Accepted for publication
12 July 2022

Q.L., Y.T., Y.H. and Ji'an Wang contributed equally.

*Plain language summary available online

DOI 10.1111/bjd.21783

Abstract

Background The key pathophysiological changes in androgenetic alopecia (AGA) are limited to hair follicles (HFs) in frontal and vertex regions, sparing the occipital region.
Objectives To identify biological differences among HF subpopulations.
Methods Paired vertex and occipital HFs from 10 male donors with AGA were collected for RNA sequencing assay. Furthermore, HF and cell experiments were conducted on the identified key genes to reveal their roles in AGA.
Results Transcriptome profiles revealed that 506 mRNAs, 55 microRNAs and 127 long noncoding RNAs were differentially expressed in the AGA vertex HFs. Pathway analysis of mRNAs and microRNAs revealed involvement of the hypoxia-inducible factor (HIF)-1, Wnt/β-catenin, and focal adhesion pathways. Differential expression of HIF-1 prolyl hydroxylase enzymes (*EGLN1*, *EGLN3*) and Wnt/β-catenin pathway inhibitors (*SERPINF1*, *SFRP2*) was experimentally validated. *In vitro* studies revealed that reduction of *EGLN1*, *EGLN3*, *SERPINF1* and *SFRP2* stimulated proliferation of dermal papilla cells. *Ex vivo* HF studies showed that downregulation of *EGLN1*, *EGLN3* and *SERPINF1* promoted HF growth, postponed HF catagen transition, and prolonged the anagen stage, suggesting that these genes may be potentially utilized as therapeutic targets for AGA.
Conclusions We characterized key transcriptome changes in male AGA HFs, and found that HIF-1 pathway-related genes (*EGLN1*, *EGLN3*) and Wnt pathway inhibitors (*SERPINF1*, *SFRP2*) may play important roles in AGA.

What is already known about this topic?

- Multiple differentially expressed genes and signalling pathways have been found between hair follicles (HFs) in the balding area (frontal and vertex regions) and nonbalding area (occipital region) of individuals with androgenetic alopecia (AGA).
- A whole-transcriptome atlas of the vertex and occipital region is lacking.

What does this study add?

- We identified a number of differentially expressed genes and pathways between balding vertex and nonbalding occipital AGA HFs by using whole-transcriptome analyses.
- We identified pathways not previously reported in AGA, such as the hypoxia-inducible factor (HIF)-1 signalling pathway.
- We verified that HIF-1 pathway-related genes (*EGLN1*, *EGLN3*) and Wnt pathway inhibitors (*PEDF*, *SFRP2*) played important roles in dermal papilla cell activity, hair growth and the hair cycle.

What is the translational message?

- The *EGLN1*, *EGLN3*, *SERPINF1* and *SFRP2* genes may be potentially utilized as therapeutic targets for AGA.

Androgen alopecia (AGA), or male pattern hair loss, is the most common type of progressive hair loss.[1] It often becomes a psychological burden and affects the normal social life of affected individuals.[2] Currently, minoxidil and finasteride are the only two drugs that have obtained approval from the US Food and Drug Administration (FDA) for AGA treatment. In addition to a scarcity of pharmacological approaches, alopecia can also be treated with various hair loss strategies, including hair transplants and germinal caps.

In normal adults, hair follicles (HFs) undergo a lifelong cyclical transformation, progressing through stages of rapid growth (anagen), regression (catagen) and relative quiescence (telogen).[3] However, in AGA, due to the effect of the testosterone metabolite dihydrotestosterone on susceptible HFs, the anagen phase of HFs is gradually reduced while the telogen phase is prolonged.[4,5] This change results in HF miniaturization,[6] leading to a transformation from terminal to vellus-like hair in individuals with AGA. As the acknowledged target, dermal papillae (DPs) are the main sites of androgen activity in HFs.[7,8] The miniaturization seen in the patterned hair loss may be the direct result of the reduction in the number of dermal papilla cells (DPCs) and, hence, in the size of the DPs.

In male AGA, hair loss typically involves the temporal and vertex region, generally sparing the occipital region.[9] Several gene expression profiling studies have identified differences in the expression levels of genes and signalling pathways between HFs in the balding area (i.e. frontal and vertex regions) and nonbalding area (i.e. occipital region) of individuals with AGA,[10,11] including androgen metabolism, the Wnt/β-catenin pathway, and redox state.[12–18] However, these studies only detected the mRNA alterations while the changes of other noncoding RNAs were neglected. Moreover, previous transcriptome studies mainly focused on plucked HFs, resulting in damage of key cell types in AGA, including DPCs and the bulge region cells.[19]

To further explore the pathogenesis of AGA, we performed a whole-transcriptome analysis to identify the differentially expressed mRNAs, microRNAs (miRNAs) and long noncoding RNAs (lncRNAs) in HF subpopulations. The HFs in balding vs. nonbalding scalp were obtained by follicular unit extraction so they would consist of more key cell types from the same male patients with AGA in our study. Furthermore, we conducted follow-up *in vitro* and *ex vivo* experiments to verify and reveal the roles of identified genes and pathways in AGA pathogenesis.

Materials and methods

Human hair follicle organ dissection

All male participants with AGA signed informed consent and were notified about the study before participation. The study was approved by Huashan Hospital of Fudan University (ethical approval number 2019M-008). The clinical information of the study participants is shown in Table S1 (see Supporting Information). Samples from patients 1–10 were used for RNA sequencing and those from patients 1–20 were used for the follow-up functional studies. Anagen HFs in the vertex and occipital areas from male patients with AGA undergoing hair transplants were collected by follicular unit extraction, and haematoxylin and eosin staining was performed to confirm the hair cycle stage (Figure S1; see Supporting Information). Anagen follicles were used in this study and were used in RNA sequencing analysis and *ex vivo* HF studies.

RNA sequencing and bioinformatic analysis

The parameters, reagents and methods for sequencing and bioinformatic analysis can be found in Appendix S1 (see Supporting Information).[20–28]

Human hair follicle culture and treatment

The isolated human HFs were cultured in Williams E medium (Gibco BRL, Grand Island, NY, USA). HFs that grew to lengths

of 0·3–0·5 mm and macroscopically remained in anagen VI after 24 h were selected for further experiments.[29] For transfection experiments, HFs were transfected with 0·04 nmol L^{-1} *EGLN1*, *EGLN3*, *SFRP2* or *SERPINF1* (formerly *PEDF*) small interfering (si)RNA mixed with 2 μmol L^{-1} Lipofectamine RNAiMAX transfection reagent (Thermo Fisher Scientific, Waltham, MA, USA). The transfection effect was evaluated at 2 days post-transfection by immunofluorescence. For recombinant protein stimulation experiments, HFs were incubated with 100 ng mL^{-1} recombinant pigment epithelium-derived factor (PEDF) protein (HY-P7054; MedChemExpress, Monmouth Junction, NJ, USA) or 1 μg mL^{-1} recombinant secreted Frizzled-related protein 2 (SFRP2) protein (6838-FR-025; R&D Systems Inc., Minneapolis, MN, USA). The length of the hair shaft and the hair cycle were measured every 2 days.

Immunofluorescence staining

HF samples were embedded in paraffin. Next, histological sections were incubated overnight at 4 °C with primary antibodies for either EGLN1 (1 : 300, sc-271835; Santa Cruz Biotechnology, Santa Cruz, CA, USA), EGLN3 (1 : 250, ab184714; Abcam, Cambridge, UK), PEDF (1 : 500, ab180711; Abcam) or SFPR2 (1 : 500, ab92667; Abcam). The sections were then incubated with the corresponding secondary antibody for 1 h at room temperature. After removing the secondary antibody, the nucleus was counterstained with 4-amino-6-diamino-2-phenylindole (DAPI; Beyotime Biotech, Nanjing, China). The stained sections were observed under a microscope (Olympus, Tokyo, Japan), and representative images were captured.

Real-time polymerase chain reaction

DPCs were isolated from HF bulbs and cultured in Dulbecco's modified Eagle's medium as previously reported.[30] Total RNA was extracted and reverse transcribed from HFs or DPCs using TRIzol (Invitrogen, Carlsbad, CA, USA) and the High Capacity cDNA Reverse Transcription Kit (Applied Biosystems, Foster City, CA, USA). Real-time polymerase chain reaction (PCR) was performed with SYBR Premix Ex Taq (Takara Bio, Shiga, Japan) and analysed with an ABI Prism 7900 Detector System (Applied Biosystems). The housekeeping gene *GAPDH* was used as the endogenous control.

Real-time cellular analysis assay

Real-time cellular analysis (Agilent, Santa Clara, CA, USA) was applied to monitor cell viability according to the manufacturer's instructions. An xCELLigence system (Roche Applied Science, Penzberg, Germany) was used to record the cell growth curves automatically. Cell index was used to observe cell state (e.g. cell attachment, cell number). Cells at a density of 9000 cells per well were seeded in a 16-well microplate. After incubation for 6 h, the medium was refreshed with new treatment medium.

Western blot

Cell lysates were subjected to sodium dodecyl sulfate polyacrylamide gel electrophoresis and proteins were transferred onto polyvinylidene fluoride (PVDF) membranes. According to the standard protocol, the PVDF membranes were blocked in Tris-buffered saline with Tween (TBST, pH 7·4) and 5% bovine serum albumin for 2 h and incubated with their respective primary antibodies for 8 h at 4 °C, followed by the secondary antibody for 2 h at room temperature. After washing with TBST three times, the proteins were visualized using the ECL chemiluminescence system (Santa Cruz Biotechnology). ImageQuant TL software (Cytiva, Marlborough, MA, USA) was used to quantify the intensity of bands.

Deferoxamine treatment

Deferoxamine was purchased from Sigma-Aldrich (St Louis, MO, USA). The working concentration for treatment of DPCs was 300 ng mL^{-1}. RNA and protein were extracted from DPCs after 24-h and 48-h incubation periods with or without deferoxamine, respectively.

Statistical analysis

All data were analysed using R (v3.6.0; R Foundation, Vienna, Austria). The paired-sample t-test and unpaired-sample t-test were used for paired samples and unpaired samples, respectively. *P*-values $< 0·05$ following false discovery rate adjustment for multiple testing correction were considered to be statistically significant.

Results

Whole-transcriptome signatures of hair follicles from individuals with androgenetic alopecia

To explore the pathogenesis of AGA, we performed RNA sequencing of protein-coding genes, lncRNAs and miRNAs in paired HFs of the frontal vertex and occipital scalp from 10 male patients with AGA (Figure S1). The whole-genome transcriptomic profiles of these two groups were pooled together and presented as a circle plot based on their *P*-values and the chromosome location of each gene (Figure 1a). Differential expression analysis identified 506 mRNAs, 127 lncRNAs and 55 miRNAs that were differentially expressed. Hierarchical clustering indicated that most mRNAs and miRNAs were upregulated in the vertex group compared with the occipital group (Figure 1b, c), whereas lncRNAs were mainly downregulated (Figure S2a; see Supporting Information). For the differentially expressed mRNAs, 308 genes were upregulated, and 198 downregulated genes were identified in the vertex group (Figure 1d). In miRNAs, we identified 35 upregulated miRNAs and 20 downregulated miRNAs (Figure 1e). We also detected 53 upregulated lncRNAs and 74 downregulated lncRNAs (Figure S2b).

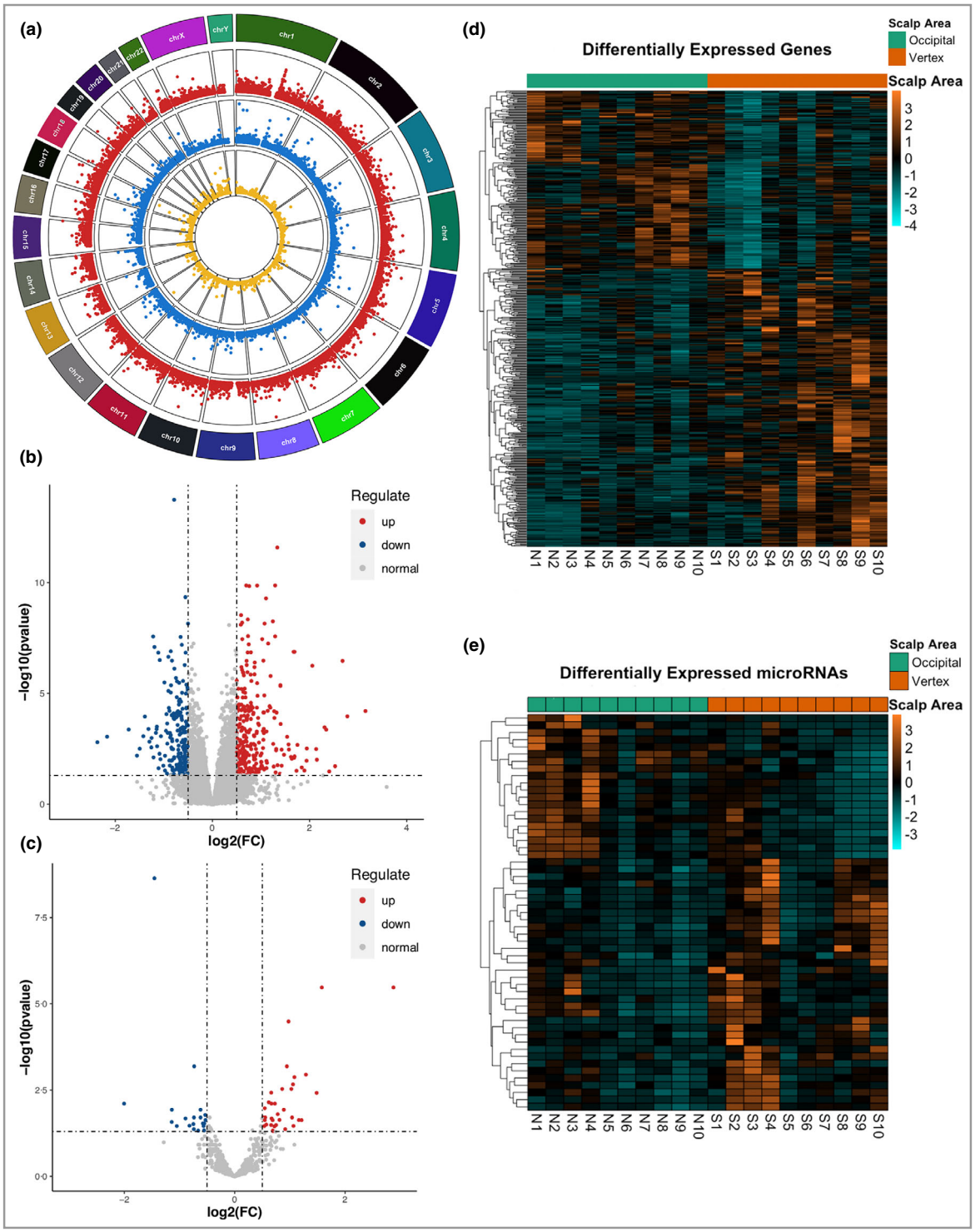

Figure 1 The whole-genome transcriptional signature of human hair follicles of patients with androgenetic alopecia (AGA). (a) Circle plot showing the results of the integration of transcriptomic data on hair follicle mRNA (red, outer circle), long noncoding RNA (blue, middle circle) and microRNA (yellow, inner circle) with their P-values from the DESeq2 results. (b, c) Differential expression analyses of (b) mRNAs and (c) microRNAs are shown in the volcano plots. Each dot represents either an expressed mRNA gene or mature microRNA. The red dots represent overexpression in the vertex group and the blue dots indicate downregulation after screening with false discovery rate correction for multiple testing (FDR $< 0{\cdot}05$) and $\log_2$ fold change ($< -0{\cdot}5$ or $> 0{\cdot}5$). (d, e) Hierarchical clustering analysis of differentially expressed (d) mRNAs and (e) microRNAs of 10 patients with AGA. Each column shows the gene expression value of one sample, and each row represents one gene in the model. Orange and blue indicate high and low *z*-scored levels, respectively, while red and green on the legend bar represent hair follicles from the vertex and occipital scalp, respectively.

These results showed significantly differential expression patterns between vertex and occipital HFs in AGA. The details of the differentially expressed genes, miRNAs and lncRNAs are listed in Tables S2–4 (see Supporting Information). In addition, we identified the correlation pairs of differentially expressed RNAs through correlation analysis and constructed regulatory networks using these correlation pairs. The lncRNA–mRNA coexpression networks and miRNA–mRNA and miRNA–lncRNA regulatory networks were constructed based on their coefficients using Cytoscape[28] (Figure S3a–c; see Supporting Information). Moreover, a competitive endogenous RNA network was constructed to identify the key regulators using miRNA–mRNA and miRNA–lncRNA pairs (Figure S3d). The results of the coexpression analysis are presented in Tables S5–7 (see Supporting Information).

Pathway enrichment analysis: hypoxia-inducible factor-1 and Wnt signalling pathways

We further performed KEGG pathway enrichment analysis to identify the altered signalling pathways in AGA. We found that the upregulated mRNAs in AGA vertex HFs were significantly enriched in the HIF-1 signalling pathway (adjusted $P = 9{\cdot}8 \times 10^{-7}$). The downregulated mRNAs were mainly enriched in the Wnt signalling pathway (adjusted $P = 7{\cdot}9 \times 10^{-5}$) and Hippo signalling pathway (adjusted $P = 8{\cdot}1 \times 10^{-5}$) (Figure 2a). The expression of key HIF-1 signalling genes (*EGLN1*, *EGLN3*, *SERPINE1*, *HMOX1*, *TIMP1*, and *IL6R*) and Wnt signalling-related genes (*SERPINF1*, *SFRP2*, *DKK1*, *LGR4*, *LGR5*, *WNT3A*, *WNT5A* and *WNT16*) is shown in Figure 2(b–d). Furthermore, Gene Ontology enrichment analysis revealed that adaptive immune response, moulting cycle, hair cycle, extracellular matrix, cytokine receptor activity, DNA-binding transcription activator activity, and hormone activity pathways were dysfunctional in balding HFs (Tables S8–10; see Supporting Information).

We also performed miRNA pathway enrichment analysis using miRPathDB.[20,23] We found that the HIF-1 and Wnt signalling pathways (data not shown) were significantly enriched with differentially expressed miRNAs using KEGG and WIKI pathway analysis, respectively (Figure 2e). In particular, the target genes of miR-451a, miR-98-5p and miR-196b-5p were significantly enriched in the HIF-1 signalling pathway (Figure 2f). In addition, the focal adhesion, cell cycle, DNA damage response and transforming growth factor-β signalling pathways were highly involved. These miRNA-enriched pathways were coordinated with mRNA-enriched pathways, which emphasizes the importance of the pathways that we identified. Therefore, the HIF-1 and Wnt signalling pathways were selected for further functional studies.

Expression validation of differentially expressed genes involved in the hypoxia-inducible factor-1 and Wnt signalling pathways

To validate the expression levels of differentially expressed genes, a total of 20 AGA samples, including 10 independent pairs of HFs, and the initial 10 pairs of HFs for RNA sequencing were collected (Table S1). Haematoxylin and eosin staining showed that the obtained HFs were anagen HFs, and revealed a concomitant decrease in the maximum bulb diameter of vertex HFs compared with occipital HFs (Figure 3a). Real-time PCR was performed to assess the expression of HIF-1 pathway-related genes (*EGLN1*, *EGLN3* and *HMOX1*) and Wnt signalling pathway-related genes (*SERPINF1*, *SFRP2* and *LGR5*). The results showed that the mRNA levels of *EGLN1*, *EGLN3*, *SERPINF1* and *SFRP2* were significantly higher in vertex HFs compared with occipital HFs (Figure 3b; and Figure S4a; see Supporting Information).

Moreover, immunofluorescence staining showed increased mean (SD) protein expression of *EGLN1* [1·04 (0·24) vs. 1·55 (0·35)], *EGLN3* [1·02 (0·06) vs. 2·65 (0·38)], *SERPINF1* [1·15 (0·25) vs. 1·75 (0·18)] and *SFRP2* [1·16 (0·21) vs. 2·54 (0·53)] in vertex HFs (Figure 3c). These proteins were ubiquitously expressed in almost every cell type, and *EGLN1* was mainly expressed in hair matrix cells (Figure 3c). Collectively, we discovered that HIF-1 and Wnt signalling pathway-related genes (*EGLN1*, *EGLN3*, *SERPINF1* and *SFRP2*) were upregulated in AGA vertex HFs and might play important roles in AGA.

The effects of hypoxia-inducible factor-1 pathway-related *EGLN1* and *EGLN3* on dermal papilla cells and hair follicles

DPC proliferation activity, HF growth and the hair cycle play important roles in the process of HF miniaturization and AGA. To assess the effects of HIF-1 pathway-related genes (*EGLN1* and *EGLN3*) in AGA, we treated DPCs and cultured HFs with *EGLN1* or *EGLN3* siRNA. Real-time PCR analysis confirmed the decreased expression of *EGLN1* or *EGLN3* after corresponding siRNA transfection into cultured DPCs (Figure 4a). Cell proliferation activity was examined by the xCELLigence system as reported,[31] and we found that downregulation of *EGLN1* or *EGLN3* resulted in a significant increase in DPC proliferation (Figure 4b). Furthermore, the decreased expression of *EGLN1* and *EGLN3* in treated HFs was confirmed by immunofluorescence (Figure 4c). As shown in Figure 4d, *EGLN1* or *EGLN3* knockdown increased the length of hair shafts compared with the negative control. Moreover, a greater percentage of anagen HFs and a lower percentage of catagen HFs remained in the *EGLN1* or *EGLN3* siRNA-treated group compared with the negative control group after 6 days of culture (Figure 4e). The results revealed that *EGLN1* or *EGLN3* downregulation promoted DPC proliferation and HF growth, prolonged the anagen stage, and postponed HF catagen transition, suggesting the important role of *EGLN1* and *EGLN3* in AGA.

The effects of Wnt pathway-related *SFRP2* and *SERPINF1* on dermal papilla cells and hair follicles

The Wnt signalling pathway plays a key role in AGA, but the effect of *SFRP2* or *SERPINF1* has not been studied in AGA. Here, we show that *SFRP2* or *SERPINF1* siRNA treatment reduced the

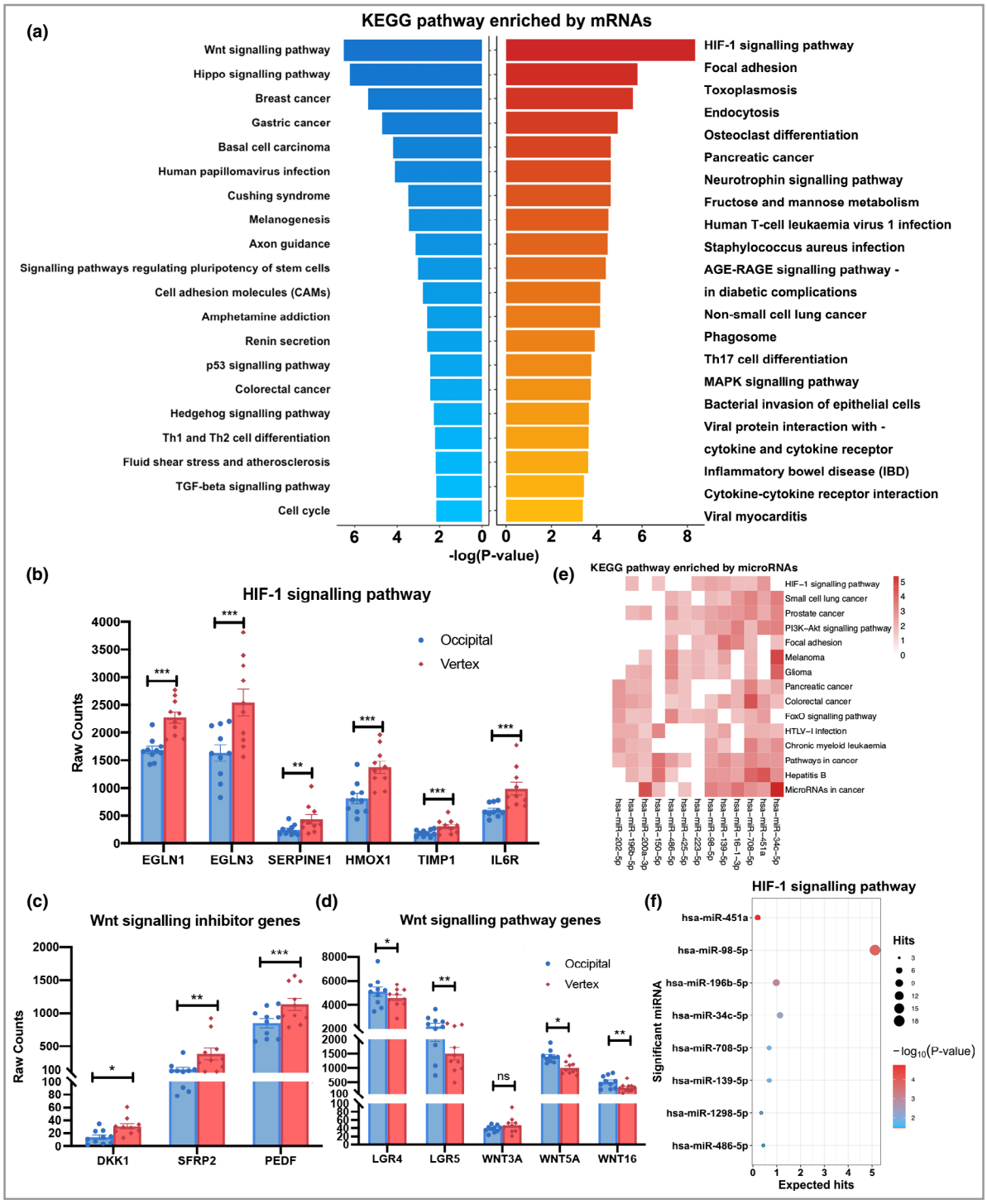

Figure 2 Enrichment of the hypoxia-inducible factor (HIF)-1 and Wnt signalling pathways. (a) KEGG pathway enrichment analysis of differentially expressed (DE) mRNAs. The red and blue bars indicate enriched pathways using the upregulated and downregulated genes in the vertex group, respectively. (b–d) Expression levels of HIF-1 signalling-related genes, Wnt signalling inhibitor genes and Wnt signalling pathway genes, respectively. The *y*-axis represents the row counts of each gene calculated by kallisto and tximport software. *P*-values were derived by DESeq2 following false discovery rate correction for multiple testing. Data are shown as the mean and SEM ($n = 10$) of each group. ***$P < 0{\cdot}001$; **$P < 0{\cdot}01$; *$P < 0{\cdot}05$; ns, not significant. (e) KEGG pathways enriched by each DE microRNA. The hypergeometric test was used to identify the enriched pathways by using the targeted genes of each DE microRNA. The legend bar represents the $-\log_{10}$(P-value) of the enriched pathway for each DE microRNA. (f) Dot plot showing that the HIF-1 signalling pathway is significantly enriched by eight DE microRNAs. The dot size represents the number of microRNA target genes belonging to the HIF-1 signalling pathway. The *x*-axis (expected hits) represents the expected number of microRNA target genes belonging to the HIF-1 signalling pathway by chance.

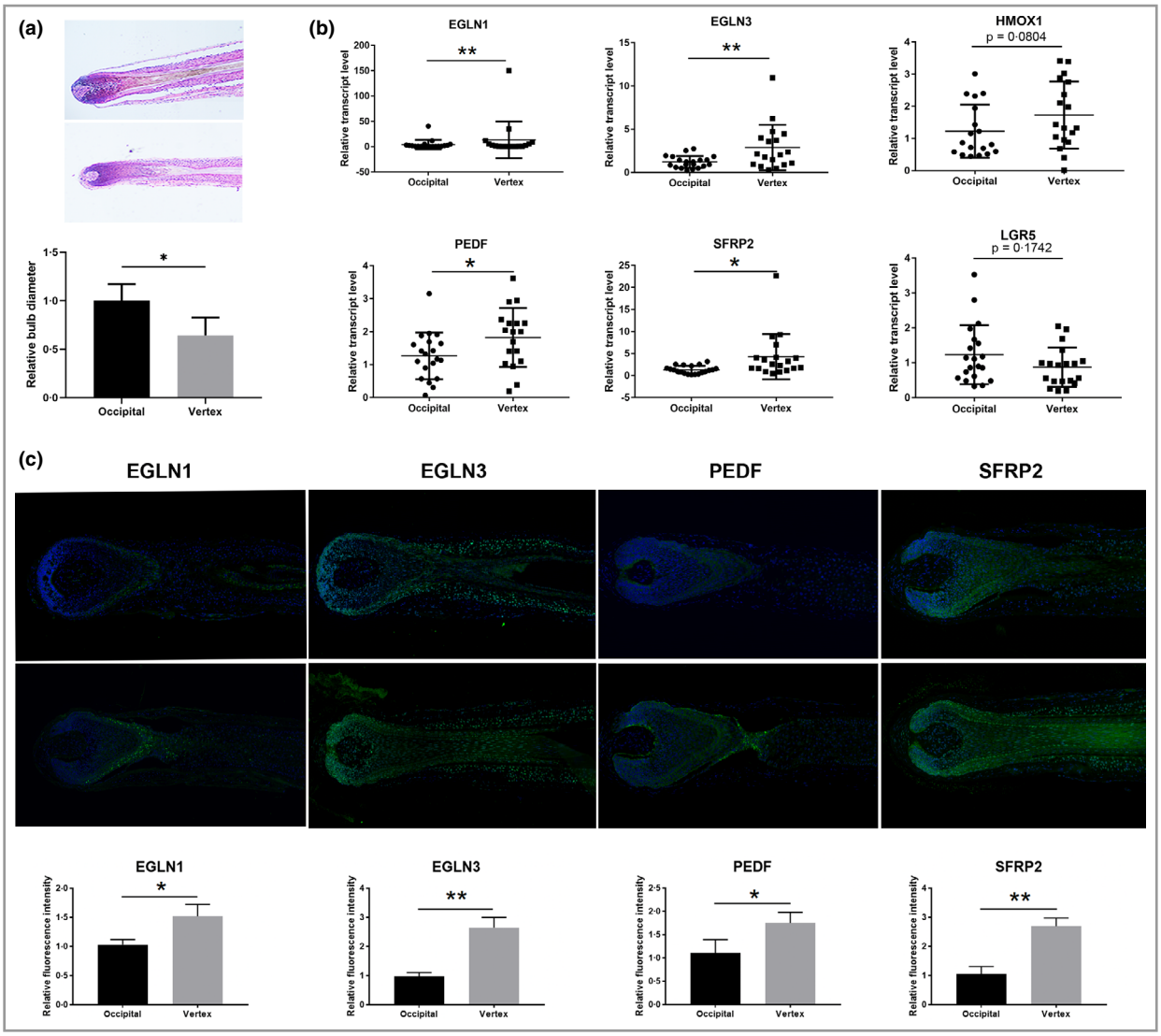

Figure 3 Validation of the expression of differentially expressed genes involved in the hypoxia-inducible factor (HIF)-1 and Wnt signalling pathways. (a) Haematoxylin and eosin staining showed that the hair follicles (HFs) were anagen HFs and the bulb diameter was decreased in vertex HFs compared with occipital HFs. (b) The expression of HIF-1 pathway-related genes (*EGLN1*, *EGLN3* and *HMOX1*) and Wnt signalling pathway-related genes (*PEDF*/*SERPINF1*, *SFRP2* and *LGR5*) was examined in vertex HFs compared with occipital HFs. The mRNA expression of *EGLN1*, *EGLN3*, *PEDF*/*SERPINF1* and *SFRP2* was significantly higher in the vertex HFs compared by paired-sample t-tests. (c) Immunofluorescence staining showed increased protein expression of EGLN1, EGLN3, PEDF or SFRP2 in vertex HFs compared by paired-sample t-tests. $^{**}P < 0{\cdot}01$, $^{*}P < 0{\cdot}05$.

transcriptomic levels of targeted genes (Figure 5a) and significantly promoted DPC proliferation (Figure 5b). Consistently, addition of recombinant *SFRP2* or *SERPINF1* protein inhibited DPC proliferation (Figure 5c). In HFs, *SFRP2* or *SERPINF1* siRNA transfection decreased target protein expression as revealed by immunofluorescence (Figure 5d). In addition, *SERPINF1* downregulation promoted HF growth, while the *SERPINF1* recombinant protein significantly inhibited HF growth (Figure 5e). However, *SFRP2* siRNA or recombinant protein treatment showed no effect on HF growth (Figure 5f). Compared with the negative control group, *SERPINF1* downregulation resulted in a greater percentage of anagen HFs remaining and a lower percentage of catagen HFs, and *SERPINF1* recombinant protein facilitated catagen transition and shortened the anagen stage (Figure 5g, h). Although *SFRP2* is an inhibitor of the Wnt pathway, *SFRP2* did not significantly affect the HF hair cycle (Figure 5g, i). These findings suggest that as *SERPINF1* is an inhibitor of the Wnt pathway, its upregulation plays a role in HF pathological changes and the development of AGA.

Discussion

Dissecting the transcriptomic alterations between AGA-affected and AGA-unaffected HFs may significantly improve our understanding of AGA pathogenesis. Hochfeld *et al.* detected the

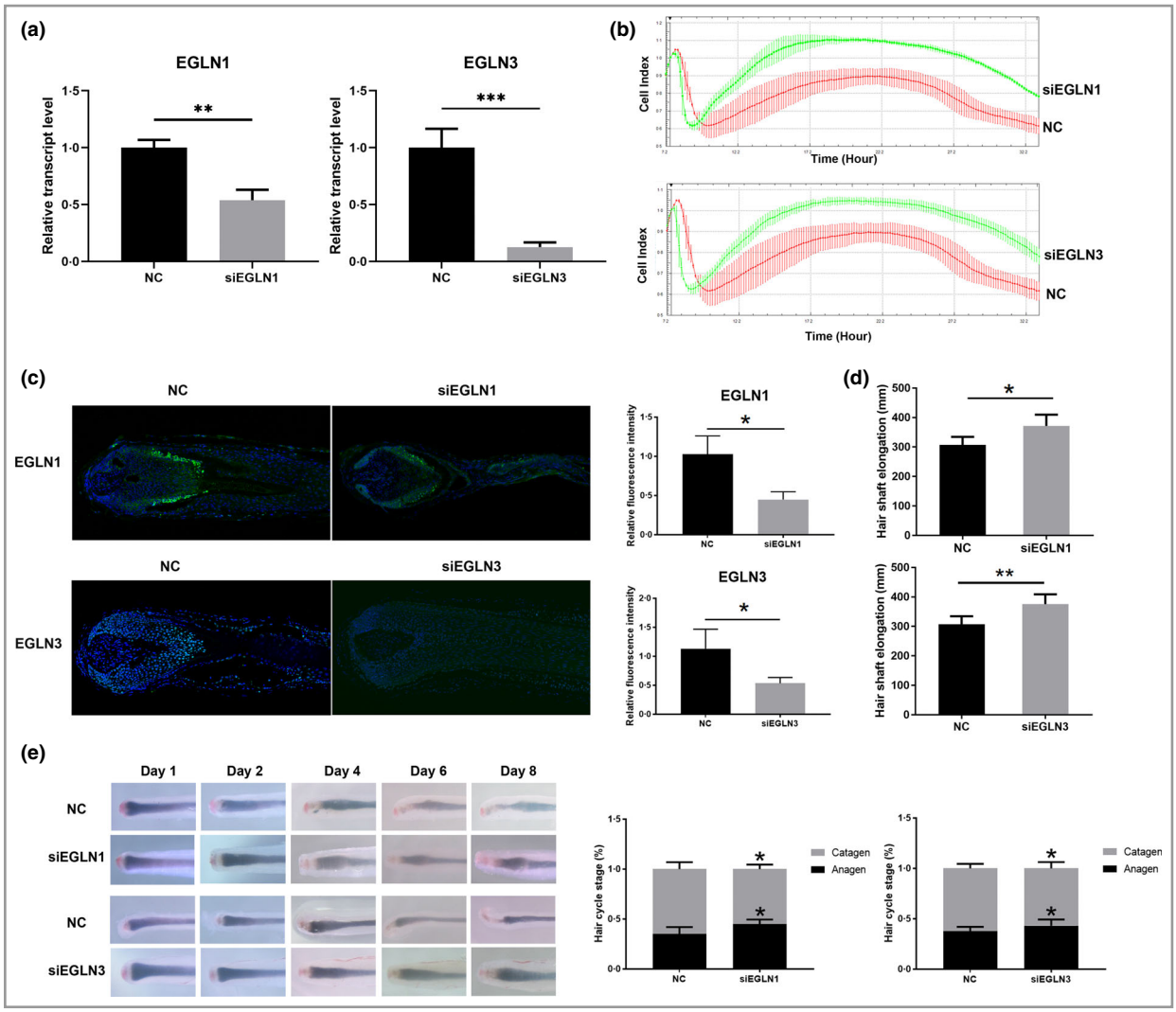

Figure 4 Effects of *EGLN1* and *EGLN3* on dermal papilla cells (DPCs) and hair follicles (HFs). (a) mRNA expression levels of *EGLN1* and *EGLN3* were significantly downregulated after corresponding small interfering (si)RNA transfection in cultured DPCs. (b) xCELLigence system detection showed that si*EGLN1* or si*EGLN3* treatment significantly increased the proliferation of DPCs compared with the negative control (NC) group DPCs. (c) Immunofluorescence staining assay identified decreased protein levels of EGLN1 and EGLN3 after si*EGLN1* or si*EGLN3* treatment of HFs. (d) *EGLN1* or *EGLN3* knockdown increased the length of hair shafts compared with the NC after 2 days of culture. (e) Macroscopic images of cultured hair follicles were obtained every other day. The hair cycle stage was macroscopically determined on day 6, and a greater percentage of anagen HFs and a lower percentage of catagen HFs remained in the *EGLN1* or *EGLN3* siRNA-treated group compared with the NC group. Data are expressed as the mean (SD) of each group. P-values were calculated using unpaired-sample t-tests. ***$P < 0{\cdot}001$, **$P < 0{\cdot}01$, *$P < 0{\cdot}05$.

transcriptomic changes between plucked HFs from the frontal and occipital scalp regions of patients with AGA, suggesting that the ephrin and Hippo signalling pathways may contribute to the deregulation of HF growth and HF miniaturization.[19] In addition, multiple miRNAs, including has-miR-106a, has-miR-106b, has-miR-125b, has-miR-221 and has-miR-410, were found to be upregulated in the balding DPCs.[32,33] Moreover, hsa-miR-133b was dysregulated in the AGA scalp and could affect the proliferation of DPCs via the Wnt/β-catenin pathway.[34] Also, has-miR-324-3p was depleted in balding follicular stem cells from patients with AGA and could affect the differentiation programme of keratinocytes.[35] However, few studies have systemically identified the transcriptomic changes of AGA HFs at the whole-transcriptome level. In this study, we have identified differentially expressed mRNA, miRNAs and lncRNAs between the male AGA HFs of the occipital and vertex regions, and highlighted the roles of the HIF-1 and Wnt/β-catenin signalling pathways in AGA pathogenesis.

The HIF-1 signalling pathway plays a crucial role in regulating cellular homeostasis under hypoxia. HIF-1 transactivates an array of gene-producing proteins capable of increasing oxygen supply, including vascular endothelial growth factor (VEGF), which promotes angiogenesis.[36,37] The HIF subunit is usually prolyl hydroxylated by EGLN (also called prolyl hydroxylase domain, PHD) family members under normoxic conditions, causing its rapid degradation. Previous studies

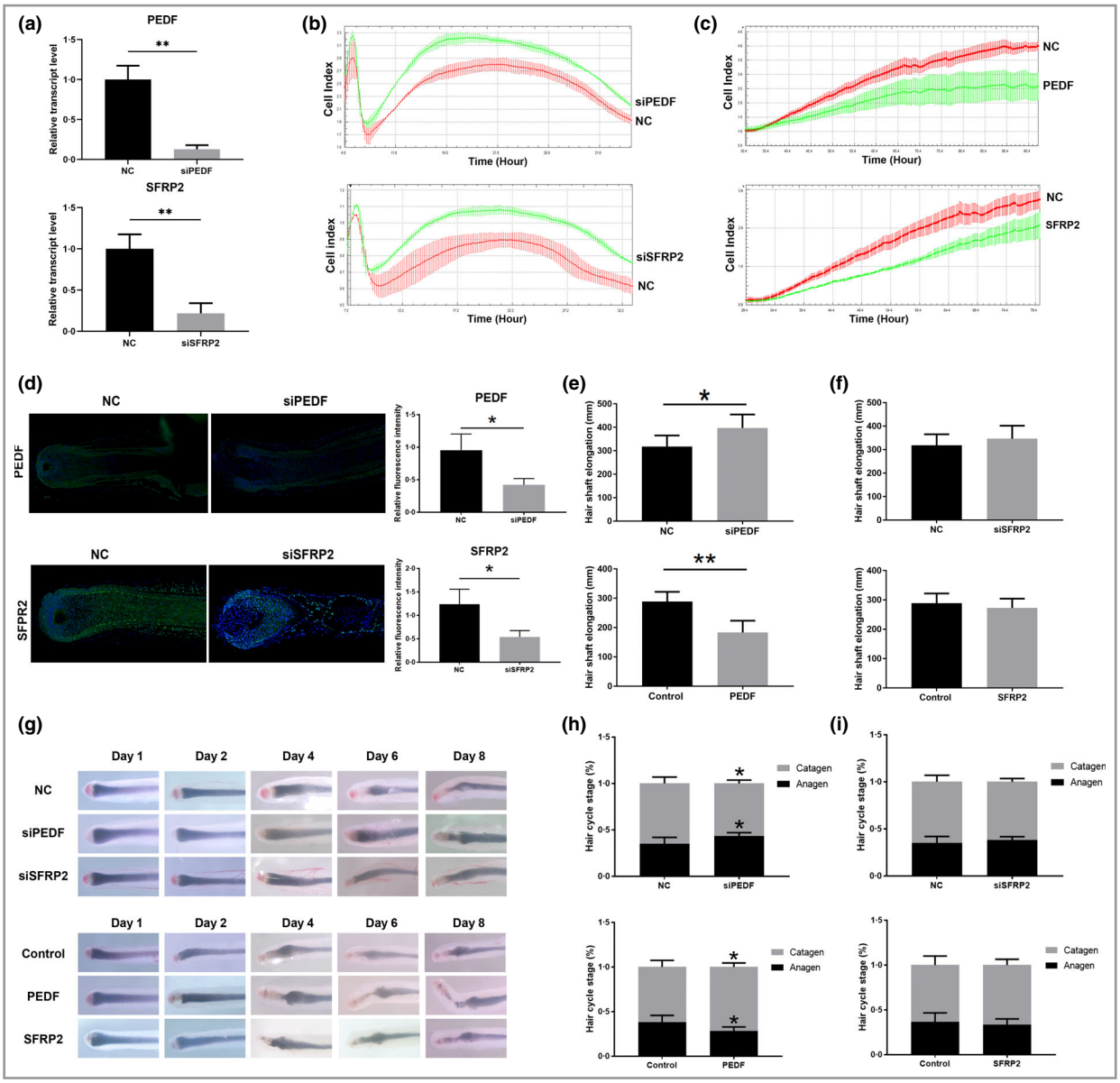

Figure 5 Effects of *PEDF/SERPINF1* and *SFRP2* on dermal papilla cells (DPCs) and hair follicles (HFs). (a) The mRNA expression levels of *PEDF/SERPINF1* and *SFRP2* were significantly downregulated after corresponding small interfering (si)RNA transfection in cultured DPCs. (b) xCELLigence system detection showed that si*PEDF/SERPINF1* or si*SFRP2* treatment significantly increased the proliferation of DPCs compared with the negative control (NC) group DPCs. (c) Recombinant protein PEDF or SFRP2 treatment decreased the proliferation of DPCs. (d) Immunofluorescence staining assay identified decreased protein levels of PEDF and SFRP2 after si*PEDF* or si*SFRP2* treatment of HFs. (e) *PEDF/SERPINF1* knockdown increased the length of hair shafts, whereas PEDF recombinant protein significantly inhibited HF growth compared with the NC after 2 days of culture. (f) Treatment with si*SFRP2* or recombinant SFRP2 protein showed no significant effect on HF growth. (g) Macroscopic images of cultured hair follicles in different groups were obtained every other day. (h, i) Quantification of hair cycle stage from macroscopic images of cultured hair follicles on day 6. A greater percentage of anagen HFs and a lower percentage of catagen HFs remained in the *PEDF/SERPINF1* siRNA-treated group, and PEDF recombinant protein facilitated catagen transition and shortened the anagen stage. By contrast, si*SFRP2* and recombinant SFRP2 showed no significant effect on the HF hair cycle. Data are expressed as the mean (SD) of each group. *P*-values were calculated using unpaired-sample t-tests. $^{**}P < 0{\cdot}01$, $^{*}P < 0{\cdot}05$.

have reported that hair loss, including AGA, is strongly associated with a reduced vascularization of HFs.[38] Minoxidil, an FDA-approved drug for AGA treatment, may activate the HIF-1–VEGF pathway, and PHD may be the molecular target for minoxidil-mediated VEGF induction via HIF-1 in keratinocytes and DPCs.[39] A combination of pyridine-2,4-dicarboxylic acid diethyl ester and resveratrol, which stabilizes HIF-1α and reduces oxygen peroxide-induced oxidative stress, improved hair density in females donors.[40] Moreover, our study also found that downregulation of *EGLN1* or *EGLN3* could stimulate

DPC proliferation and promote HF growth. Therefore, we suggest that *EGLN1* or *EGLN3* may regulate DPC and HF growth through the HIF-1–VEGF pathway.

To further verify this assumption, we first confirmed the decreased expression and protein levels of HIF-1α and VEGFA in the vertex HFs of patients with AGA (Figure S4b, c), and found they could be restored after si*EGLN1* or si*EGLN3* treatment (Figure S4d). In accordance, expression and protein levels of HIF-1α and VEGFA could be upregulated after si*EGLN1* or si*EGLN3* treatment in DP cells (Figure S5a–d; see Supporting Information). Furthermore, DP cells treated with deferoxamine (an iron chelator) could also upregulate transcriptomic and protein levels of HIF-1α and VEGFA, resulting in a higher proliferation of DP cells (Figure S5e–g). Taking the results together, we suggest that *EGLN1* and *EGLN3* may regulate HF DPs and HFs through the HIF-1–VEGF signalling pathway. However, a previous study found that loss of *EGLN1* could activate the HIF-dependent hypoxic response, including anaerobic glycolysis,[41] suggesting that EGLN1 and EGLN3 might regulate HF metabolism to participate in AGA pathogenesis. In addition, we only examined the role of EGLN1 and EGLN3 in DP cells, and the effect of EGLN1 and EGLN3 on HF epithelial cells remains elusive. Further investigations are required to clarify the diverse effects of EGLN1 and EGLN3 on different compartments of HFs.

Wnt/β-catenin signalling plays a pivotal role in HF morphogenesis, development and regeneration during the hair cycle.[12] In accordance with previous studies, we found downregulation of the Wnt signalling pathway in the vertex HFs of patients with AGA compared with occipital HFs. Targeting Wnt signalling is more likely to come from approaches that interfere with Wnt antagonists and restore signalling. Extensive research has shown that modulation of Wnt natural inhibitors, including *DKK1*, *DKK2*, *SFRP1* and *SFRP4*, could result in comparable growth-promoting effects while alleviating some safety concerns.[15,18,42–44]

In this study, we scanned the common Wnt signalling pathway inhibitor genes and found that only four of these genes (*SFRP2*, *SERPINF1*, *DKK1* and *IGFBP3*) were significantly upregulated in the AGA vertex region, and few studies have focused on the roles of *SFRP2* and PEDF in AGA. Therefore, we further examined these two Wnt signalling pathway inhibitors for follow-up experiments. We found that *SERPINF1* downregulation stimulated DPC proliferation, promoted HF growth, postponed HF catagen transition, and prolonged the anagen stage, while PEDF recombinant protein showed opposite results. SFRP2 has been widely recognized as an inhibitor of Wnt signalling, and SFRP2 downregulation can activate Wnt siganling.[45–47] However, Kwack *et al.* reported that SFRP2 could augment WNT3a-mediated Wnt signalling, suggesting that the role of SFRP2 in the Wnt signalling pathway is complex and warrants further clarification.[48] In our study, we found that exogenous *SFRP2* could inhibit DPC proliferation. However, treatment with *SFRP2* siRNA or recombinant protein showed no significant effects on HF growth, which might be due to the effects of functional *SFRP1* as previously reported.[18]

In conclusion, our study characterizes the whole-transcriptome signatures of HFs from the balding vertex and nonbalding occipital scalp areas of patients with AGA, highlighting the HIF-1 signalling pathway and Wnt/β-catenin pathway in AGA pathogenesis. We identified that HIF-1 pathway-related genes (*EGLN1* and *EGLN3*) and Wnt/β-catenin pathway inhibitors (*SFRP2* and *SERPINF1*) may play important roles in DPC activity, hair growth and the hair cycle, and may potentially be utilized as targets for AGA and hair loss treatment. Further studies with larger sample sizes are awaited to validate these findings in the future. We anticipate that our data will serve as a valuable resource facilitating future studies for patients with AGA.

Acknowledgments

We thank all of the authors for their efforts in this work and all of the participants involved in this study. Wenyu Wu, Jinran Lin and Jiucun Wang contributed equally to this work.

Funding sources

This study was supported by grants from National Science Foundation of China (82173442, 82103759), Shanghai Engineering Research Center of Hair Medicine (19DZ2250500), Clinical Research Plan of SHDC (SHDC2020CR2033B), Science and Technology Committee of Shanghai Municipality Guiding Fund (19411962400), CAMS Innovation Fund for Medical Sciences (2019-I2M-5-066), the innovative research team of high-level local universities in Shanghai, and Shanghai Municipal Science and Technology Major Project (2017SHZDZX01).

Conflicts of interest

The authors declare they have no conflicts of interest.

Data availability

The data and the code that support the findings of this study are available on reasonable request from the corresponding author.

Ethics statement

The study was approved by Huashan Hospital of Fudan University (ethical approval number 2019M-008).

Supporting Information

Additional Supporting Information may be found in the online version of this article at the publisher's website:

Appendix S1 Supplementary methods.

Figure S1 Human hair follicle organ dissection from male patients with androgenetic alopecia.

Figure S2 The transcriptomic signature of long noncoding RNAs.

Figure S3 Network analysis.

Figure S4 The activity of the hypoxia-inducible factor-1α pathway in vertex hair follicles and *EGLN1* or *EGLN3* downregulated hair follicles.

Figure S5 The effects of deferoxamine, *EGLN1* and *EGLN3* on dermal papilla cells.

Table S1 Characteristics of male patients with androgenetic alopecia in this study.

Table S2 The differentially expressed mRNAs.

Table S3 The differentially expressed microRNAs.

Table S4 The differentially expressed long noncoding RNAs.

Table S5 Results of Pearson correlation analysis: the long noncoding RNA–mRNA pairs.

Table S6 Results of Pearson correlation analysis: the microRNA–mRNA pairs.

Table S7 Results of Pearson correlation analysis: the microRNA–long noncoding RNA pairs.

Table S8 Results of Gene Ontology enrichment analysis (biologic processes).

Table S9 Results of Gene Ontology enrichment analysis (cellular components).

Table S10 Results of Gene Ontology enrichment analysis (molecular functions).

References

1 Kelly Y, Blanco A, Tosti A. Androgenetic alopecia: an update of treatment options. *Drugs* 2016; **76**:1349–64.

2 Gupta S, Goyal I, Mahendra A. Quality of life assessment in patients with androgenetic alopecia. *Int J Trichol* 2019; **11**:147–52.

3 Oh JW, Kloepper J, Langan EA *et al.* A guide to studying human hair follicle cycling *in vivo*. *J Invest Dermatol* 2016; **136**:34–44.

4 Ellis JA, Sinclair R, Harrap SB. Androgenetic alopecia: pathogenesis and potential for therapy. *Expert Rev Mol Med* 2002; **4**:1–11.

5 Sawaya ME. Purification of androgen receptors in human sebocytes and hair. *J Invest Dermatol* 1992; **98** (6 Suppl.):92S–96S.

6 Hamada K, Randall VA. Inhibitory autocrine factors produced by the mesenchyme-derived hair follicle dermal papilla may be a key to male pattern baldness. *Br J Dermatol* 2006; **154**:609–18.

7 Betriu N, Jarrosson-Moral C, Semino CE. Culture and differentiation of human hair follicle dermal papilla cells in a soft 3D self-assembling peptide scaffold. *Biomolecules* 2020; **10**:684.

8 Chew EGY, Tan JHJ, Bahta AW *et al.* Differential expression between human dermal papilla cells from balding and non-balding scalps reveals new candidate genes for androgenetic alopecia. *J Invest Dermatol* 2016; **136**:1559–67.

9 Wirya CT, Wu W, Wu K. Classification of male-pattern hair loss. *Int J Trichol* 2017; **9**:95–100.

10 Zhang M, Chen Y, Guan L *et al.* Identification of key genes and signaling pathways in male androgenetic alopecia by bioinformatics analysis. In: *Proceedings of the Fourth International Conference on Biological Information and Biomedical Engineering*, 2020. Article no. 13; doi: https://doi.org/10.1145/3403782.3403795.

11 Reinholz M, French LE. Medical education and care in dermatology during the SARS-CoV2 pandemia: challenges and chances. *J Eur Acad Dermatol Venereol* 2020; **34**:e214–16.

12 Premanand A, Reena Rajkumari B. Androgen modulation of Wnt/β-catenin signalling in androgenetic alopecia. *Arch Dermatol Res* 2018; **310**:391–9.

13 Lei MX, Chuong CM, Widelitz RB. Tuning Wnt signals for more or fewer hairs. *J Invest Dermatol* 2013; **133**:7–9.

14 Clevers H, Nusse R. Wnt/β-catenin signaling and disease. *Cell* 2012; **149**:1192–205.

15 Leirós GJ, Ceruti JM, Castellanos ML *et al.* Androgens modify Wnt agonists/antagonists expression balance in dermal papilla cells preventing hair follicle stem cell differentiation in androgenetic alopecia. *Mol Cell Endocrinol* 2017; **439**:26–34.

16 Leirós GJ, Attorresi AI, Balañá ME. Hair follicle stem cell differentiation is inhibited through cross-talk between Wnt/β-catenin and androgen signalling in dermal papilla cells from patients with androgenetic alopecia. *Br J Dermatol* 2012; **166**:1035–42.

17 Nieves A, Garza LA. Does prostaglandin D2 hold the cure to male pattern baldness? *Exp Dermatol* 2014; **23**:224–7.

18 Hawkshaw NJ, Hardman JA, Haslam IS *et al.* Identifying novel strategies for treating human hair loss disorders: cyclosporine A suppresses the Wnt inhibitor, SFRP1, in the dermal papilla of human scalp hair follicles. *PLOS Biol* 2018; **16**:e2003705.

19 Hochfeld LM, Keller A, Anhalt T *et al.* Insights into male androgenetic alopecia: differential gene expression profiling of plucked hair follicles and integration with genetic data. *J Invest Dermatol* 2019; **139**:235–8.

20 Backes C, Kehl T, Stöckel D *et al.* miRPathDB: a new dictionary on microRNAs and target pathways. *Nucleic Acids Res* 2017; **45**:D90–6.

21 Bray NL, Pimentel H, Melsted P *et al.* Near-optimal probabilistic RNA-seq quantification. *Nat Biotechnol* 2016; **34**:525–7.

22 Gu Z, Gu L, Eils R *et al.* circlize implements and enhances circular visualization in R. *Bioinformatics* 2014; **30**:2811–12.

23 Kehl T, Kern F, Backes C *et al.* miRPathDB 2.0: a novel release of the miRNA Pathway Dictionary Database. *Nucleic Acids Res* 2020; **48**:D142–7.

24 Love MI, Huber W, Anders S. Moderated estimation of fold change and dispersion for RNA-seq data with DESeq2. *Genome Biol* 2014; **15**:550.

25 Soneson C, Love MI, Robinson MD. Differential analyses for RNA-seq: transcript-level estimates improve gene-level inferences. *F1000Res* 2015; **4**:1521.

26 Yu G, Wang LG, Han Y *et al.* clusterProfiler: an R package for comparing biological themes among gene clusters. *Omics* 2012; **16**:284–7.

27 Zhao S, Gordon W, Du S *et al.* QuickMIRSeq: a pipeline for quick and accurate quantification of both known miRNAs and isomiRs by jointly processing multiple samples from microRNA sequencing. *BMC Bioinformatics* 2017; **18**:180.

28 Shannon P, Markiel A, Ozier O *et al.* Cytoscape: a software environment for integrated models of biomolecular interaction networks. *Genome Res* 2003; **13**:2498–504.

29 Kwon OS, Oh JK, Mi HK *et al.* Human hair growth *ex vivo* is correlated with *in vivo* hair growth: selective categorization of hair follicles for more reliable hair follicle organ culture. *Arch Dermatol Res* 2006; **297**:367–71.

30 Liu Q, Shi X, Zhang Y *et al.* Increased expression of zyxin and its potential function in androgenetic alopecia. *Front Cell Dev Biol* 2021; **8**:582282.

31 Liu Q, Lu J, Lin J *et al.* Salvianolic acid B attenuates experimental skin fibrosis of systemic sclerosis. *Biomed Pharmacother* 2019; **110**:546–53.

32 Goodarzi HR, Abbasi A, Saffari M *et al.* Differential expression analysis of balding and nonbalding dermal papilla microRNAs in male pattern baldness with a microRNA amplification profiling method. *Br J Dermatol* 2012; **166**:1010–16.

33 Goodarzi HR, Abbasi A, Saffari M *et al.* MicroRNAs take part in pathophysiology and pathogenesis of male pattern baldness. *Mol Biol Rep* 2010; **37**:2959–65.

34 Deng W, Hu T, Han L *et al.* miRNA microarray profiling in patients with androgenic alopecia and the effects of miR-133b on hair growth. *Exp Mol Pathol* 2021; **118**:104589.

35 Mohammadi P, Nilforoushzadeh MA, Youssef KK *et al.* Defining microRNA signatures of hair follicular stem and progenitor cells in healthy and androgenic alopecia patients. *J Dermatol Sci* 2021; **101**:49–57.
36 Choe GS, Bae MG, Jeong JW *et al.* Hypoxia-induced angiogenesis during carcinogenesis. *J Biochem Mol Biol* 2003; **36**:120–7.
37 Han S, Huh J, Kim W *et al.* Phospholipase D activates HIF-1-VEGF pathway via phosphatidic acid. *Exp Mol Med* 2014; **46**:e126.
38 Goldman CK, Tsai JC, Soroceanu L *et al.* Loss of vascular endothelial growth factor in human alopecia hair follicles. *J Invest Dermatol* 1995; **104** (5 Suppl.):18S–20S.
39 Yum S, Jeong S, Kim D *et al.* Minoxidil induction of VEGF is mediated by inhibition of HIF-prolyl hydroxylase. *Int J Mol Sci* 2018; **19**:53.
40 Juchaux F, Sellathurai T, Perrault V *et al.* A combination of pyridine-2,4-dicarboxylic acid diethyl ester and resveratrol stabilizes hypoxia-inducible factor 1-alpha and improves hair density in female volunteers. *Int J Cosmet Sci* 2020; **42**:167–73.
41 Suhara T, Hishiki T, Kasahara M *et al.* Inhibition of the oxygen sensor PHD2 in the liver improves survival in lactic acidosis by activating the Cori cycle. *Proc Natl Acad Sci USA* 2015; **112**:11642–7.
42 Mahmoud EA, Elgarhy LH, Hasby EA *et al.* Dickkopf-1 expression in androgenetic alopecia and alopecia areata in male patients. *Am J Dermatopathol* 2019; **41**:122–7.
43 Heilmann–Heimbach S, Herold C, Hochfeld LM *et al.* Meta-analysis identifies novel risk loci and yields systematic insights into the biology of male-pattern baldness. *Nat Commun* 2017; **8**:14694.
44 Guo H, Xing Y, Deng F *et al.* Secreted Frizzled-related protein 4 inhibits the regeneration of hair follicles. *PeerJ* 2019; **6**:e6153.
45 Kim BK, Yoon SK. Expression of sfrp2 is increased in catagen of hair follicles and inhibits keratinocyte proliferation. *Ann Dermatol* 2014; **26**:79–87.
46 Zhu N, Lin E, Zhang H *et al.* LncRNA H19 overexpression activates Wnt signaling to maintain the hair follicle regeneration potential of dermal papilla cells. *Front Genet* 2020; **11**:694.
47 Zhao B, Chen Y, Yang N *et al.* miR-218-5p regulates skin and hair follicle development through Wnt/β-catenin signaling pathway by targeting SFRP2. *J Cell Physiol* 2019; **234**:20329–41.
48 Kwack MH, Ahn JS, Jang JH *et al.* SFRP2 augments Wnt/β-catenin signalling in cultured dermal papilla cells. *Exp Dermatol* 2016; **25**:813–15.